Journal of Power Sources 189 (2009) 624–628

Contents lists available at ScienceDirect

Journal of Power Sources

journal homepage: www.elsevier.com/locate/jpowsour

Short communication

High-performance, nano-structured $LiMnPO_4$ synthesized via a polyol method

Deyu Wang[a,*], Hilmi Buqa[b], Michael Crouzet[b], Gianluca Deghenghi[b], Thierry Drezen[b], Ivan Exnar[b], Nam-Hee Kwon[b], James H. Miners[b], Laetitia Poletto[b], Michael Grätzel[a]

[a] Laboratoire de Photonique et Interfaces, Ecole Polytechnique Fédérale de Lausanne, 1015 Lausanne, Switzerland
[b] High Power Lithium HPL SA, PSE B, Ecole Polytechnique Fédérale de Lausanne, 1015 Lausanne, Switzerland

ARTICLE INFO

Article history:
Received 31 July 2008
Received in revised form
12 September 2008
Accepted 15 September 2008
Available online 1 October 2008

Keywords:
Lithium manganese phosphate ($LiMnPO_4$)
Polyol
Li-ion battery
Nano-structured

ABSTRACT

A novel polyol synthesis was adopted to synthesize nano-structured $LiMnPO_4$. This route yields well-crystallized nanoparticles with platelet morphology that are only ~30 nm thick oriented in the *b* direction. The obtained material presented a good rate behavior and a very long cyclic life both at room temperature (RT) and 50 °C. The sample exhibited a specific capacity of 145 mAh g^{-1} at C/20, 141 mAh g^{-1} at C/10 rate and 113 mAh g^{-1} 1C rate. This represents is the highest performance results reported to date for this material. The high rate performance is ascribed to the platelet shape of the $LiMnPO_4$ as it minimizes the paths for Li diffusion. At elevated temperature (50 °C) this material demonstrated improved reversible capacity of 159 mAh g^{-1} at C/10 and 138 at 1C. The electrode retained 95% of its capacity, over 200 cycles, both at RT and 50 °C. This electrochemical stability is ascribed to the structural strength of the P–O bond and the stability of the electrolyte–$LiMnPO_4$ interface. It allows us to conclude that the impact of a possible Jahn–Teller distortion is not critical. These excellent results clarified some ambiguities on $LiMnPO_4$ as cathode materials, and demonstrate its promise for its practical application.

1. Introduction

The interest in lithium ion batteries is driven by the increased market demand for portable electronics, transportation and energy storage. A strong research effort has been focused on developing new cathode materials to replace the current $LiCoO_2$. $LiCoO_2$ represents half of the price of a Li-ion cell.

Lithium metal phosphates have recently attracted attention as potential Li-ion battery cathode materials due to their lower cost, lower toxicity, and better electrochemical and thermal stability, when compared to $LiCoO_2$ [1]. Indeed $LiFePO_4$ has been extensively investigated, and is now present in commercial cells for high power, and large format applications.

Encouraged by the success of $LiFePO_4$, lithium manganese phosphates is attracting increased attention. It has a redox potential of 4.1 V vs. Li/Li^+ [1,2]. This is ~0.65 V higher than $LiFePO_4$, promising a great energy density and lower energy cost on a cell and system level. This voltage is considered to be optimum for current electrolyte: it is high enough to maximize energy density yet within the stability limits of electrolytes based on carbonate ester solvents.

The high ionic and electronic resistance of $LiMnPO_4$ have rendered it difficult to obtain high electrochemically activity. Li et al. [3] first reported the reversible reaction of Mn(II) ↔ Mn(III) in olivine phosphate. Their material presented a reversible capacity of ~140 mAh g^{-1} at C/15 within 2.0–4.5 V vs. Li/Li^+. Although several groups have explored various methods to prepare electro-active $LiMnPO_4$, there are very few reports of performance greater than 100 mAh g^{-1} [4–10].

Toyota and HPL demonstrated that particle size reduction is essential to improve the rate performance of the $LiMnPO_4$ material [6]. Smaller particles reduce the diffusion path length for electrons and lithium ions in the cathode material, there by overcoming the low intrinsic electronic conductivity and slow lithium diffusion kinetics within the material. Using this approach, and a sol–gel synthesis, they were able to achieve 156 mAh g^{-1} at C/100, 134 mAh g^{-1} at C/10 and 80 mAh g^{-1} at C. In the present paper, we apply a novel polyol synthesis method to further nano-structure $LiMnPO_4$ [11]. This synthesis method allows us to produce material with a platelet morphology. This further shortens the pathway for Li diffusion and, thus improves rate performance. We demonstrate improved performance, achieving 141 mAh g^{-1} at C/10 and 113 mAh g^{-1} at 1C at room temperature.

The polyol synthesis method yields pure well-crystallized $LiMnPO_4$ with a controlled platelet morphology of ~30 nm. The basic idea of polyol process is dissolving of metal salts in a chelating

* Corresponding author. Tel.: +41 21 6934111; fax: +41 21 6938684.
E-mail address: deyu.wang@epfl.ch (D. Wang).

0378-7753/$ – see front matter © 2008 Elsevier B.V. All rights reserved.
doi:10.1016/j.jpowsour.2008.09.077

polyalcohol (polyol) at elevated temperatures following by controlled co-precipitation by hydrolysis at higher temperature. Commonly diethylene glycol (DEG) is used as chelating polyol. The polyol medium itself acts not only as a solvent in the process but also as a stabilizer, limiting particle growth and prohibiting agglomeration [12]. A crystal sample is acquired directly from the suspension without any further calcination necessary. In contrast to other methods, this route simplifies the producing procedure, and diminishes the necessary cost.

To date, there have been few reports of the electrochemical stability of $LiMnPO_4$ [13]. Indeed, there is considerable debate about this. On one side, the three-dimensional framework of $LiMPO_4$ is stabilized by strong covalent bonds, and one can expect the good cycle life exemplified by $LiFePO_4$. In the other side, a Jahn–Teller (JT) distortion was predicted to be unavoidable in Mn(III) [d_4: $t_{2g}^3 e_g^1$] of $MnPO_4$ [14,15]. The devastating impact of JT distortion on durability is known from other systems [2,16,17]. This paper attempts to resolve the question of electrochemical stability by cycling $LiMnPO_4$ for 200 cycles, both at room temperature and at 50 °C. The material is shown to retain ~95% of its initial capacity after 200 cycles. This cyclic data, allows us to conclude that there is minimal impact of a proposed Jahn–Teller distortion from the Mn(III) [d_4: $t_{2g}^3 e_g^1$] in $MnPO_4$. The same resilience to cycling is shown at room temperature and at 50 °C. This is due to the stability of the electrolyte–$LiMnPO_4$ interface as reported by Martha et al. [18].

In this paper, we will report the polyol synthesis method for producing nano-structured $LiMnPO_4$ with platelet morphology. We present the excellent electrochemical performance and stability of this material. Its capacity at room temperature reached 141 mAh g^{-1} at C/10 and 113 mAh g^{-1} at 1C. Furthermore, our material exhibited 95% of its initial capacity after 200 cycles at ambient temperature and at 50 °C.

2. Experimental

The $LiMnPO_4$ was prepared using the following polyol synthesis. (All chemicals were used directly without further purification.) 0.06 mol manganese acetate tetra hydrate ($Mn(CH_3COO)_2{\cdot}4H_2O$, Acros, 99%) was dissolved into 30 ml deionized water and poured into 200 ml diethylene glycol (DEG, Aldrich, 99%) in a three-neck round-bottom flask. This DEG–H_2O solution was vigorously stirred and heated to over 100 °C, kept for 1 h, and then 30 ml 2 mol L^{-1} lithium dihydrogen phosphate (LiH_2PO_4, 99%, Aldrich) aqueous solution was dropped into this system with a speed of 1 ml min^{-1}. Finally the DEG suspension was kept for another 4 h at this temperature. After cooled down to room temperature, the $LiMnPO_4$ material was separated by centrifugation and washed three times with ethanol in order to remove the residual DEG and organic remnants. As a final step the material was dried in an oven at 120 °C overnight.

The electrodes containing the $LiMnPO_4$ were prepared using the following procedure: Polyol synthesized $LiMnPO_4$, was milled with 20 wt% of carbon black to obtain a carbon–$LiMnPO_4$ (C–$LiMnPO_4$) composite. A slurry of *N*-methyl pyrrolidone (NMP) was prepared containing the C–$LiMnPO_4$ composite (90.5 wt%) with poly(vinylidene fluoride) (PVdF) binder (7.5 wt%) and graphite (2 wt%). The slurry was then cast on an aluminum current collector. After drying at 140 °C under vacuum the electrodes were punched into 23 mm Ø disks and pressed at 2 tons cm^{-2}. The final electrodes have an active layer thickness of 30–55 μm with an active material loading of 5–6 mg cm^{-2}. The electrodes were subsequently assembled into a Swagelok™ fitting using Li metal foil as the counter electrode with a microporous polymer separator (Celgard 2340™) and liquid electrolyte mixtures containing 1 M $LiPF_6$ and a solvent mixture of propylene carbonate (PC), ethlylene carbonate (EC) and dimethyl carbonate (DMC) (1:1:3 v/v/v). The assembly of the test cells was performed in an M-Braun glove box filled with pure argon.

The electrochemical evaluations were conducted on an Arbin BT 2000 electrochemical measurement system under room temperature and 50 °C. The cells for rate tests were cycled between 2.70 V and 4.40 V vs. Li/Li^+. In the first cycle, the cells were charged with a C/20 rate to 4.4 V, kept at 4.4 V until C/100 rate, then discharged to 2.7 V at C/20 (=7.5 mA g^{-1}). In subsequent cycles, the cells were charged at C/10 until 4.4 V, kept at 4.4 V to C/100, then discharged at specific rate (1C = 150 mA g^{-1}). In the electrochemical stability experiments, the cells were cycled between 2.70 V and 4.25 V vs. Li/Li^+. At ambient temperature, all cycles were charged as 1C to 4.25 V, and kept until C/100. They were discharged at 1C to 2.7 V. Every 10 cycles the cells were discharged at C/10 to 2.7 V and CV discharged to C/100. At 50 °C, the cells were charged at C/5 to 4.25 V and then discharged at 5C to 2.7 V. The electrochemical capacity of samples was evaluated on the active material.

The phase of our material was characterized by X-ray diffraction (XRD) with Cu Kα radiation (Kristalloflex 805, Siemens). Its morphology was observed with field-emission scanning electron microscopy (FESEM, Philips XL30 FEG). Its microstructure was examined by transmission electron microscopy (TEM) on a Philips CM 300 equipped with a field emission gun at an accelerating voltage of 300 kV.

3. Results and discussion

X-ray diffraction pattern of the $LiMnPO_4$ material after polyol preparation is shown in Fig. 1. In comparison to the reference data (PDF reference number 704375), our sample is a pure phase $LiMnPO_4$ with olivine structure indexed in Pnma of orthorhombic system. The lattice parameters obtained from Rietveld refinement is a = 10.443 Å, b = 6.101 Å and c = 4.741 Å. SEM images of the material are provided in Fig. 2 and show that the material processes a platelet structure. The TEM image in Fig. 3 demonstrates that the platelet is 20–30 nm thick. The TEM images also show that the particles are mono-crystalline.

It is also noticed that the relative intensity of diffraction peaks was changed in our polyol materials. In standard spectrum, the highest peak is corresponding (3 1 1) panel, and the ratio of (0 2 0) and (3 1 1) is 0.78. XRD patterns of solid samples closely matched

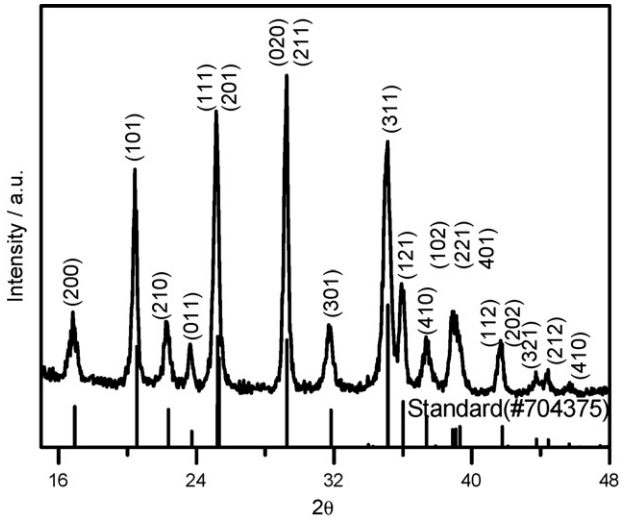

Fig. 1. XRD pattern of our material. Reference pattern (PDF#: 704375) was shown, as well.

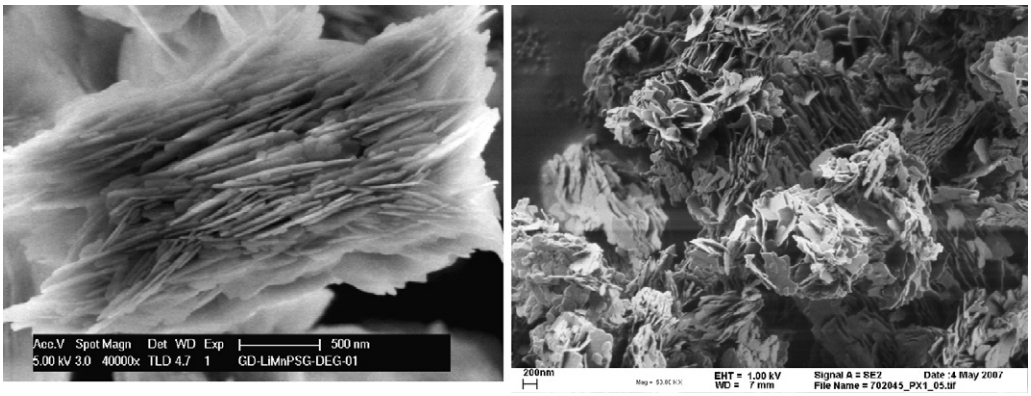

Fig. 2. SEM images of prepared sample.

this data. In our materials, (0 2 0) panel presents the strongest intensity. It is 1.28 times stronger than the peak of (3 1 1) panel. This change indicates the platelet orientated in the *a*–*c* plane. It is interesting as only the *ac* plane is active for Li extraction and insertion: Li is constrained to move only parallel to *b*. As such, this morphology is optimal for rapid ionic diffusion and good kinetics of (de)lithiation.

The electrochemical performance of the $LiMnPO_4$ was characterized at different discharging rates under RT and 50 °C. Fig. 4 shows its charge–discharge profiles at C/10. This sample exhibited a reversible plateau around 4.1 V vs. Li/Li^+, which is the typical redox potential of Mn(II) ↔ Mn(III) in olivine manganese phosphate. The material demonstrates a reversible capacity of 145 mAh g^{-1} at C/20 and 141 mAh g^{-1} at C/10 RT. This is the best performance reported to date at this rate. At 50 °C, the sample achieves 159 mAh g^{-1}. This is close to its theoretical limitation (171 mAh g^{-1}). Moreover, our composite displayed good rate behavior in both temperatures (Fig. 5). At 1C, it retained 113 mAh g^{-1} (80%) under RT and 138 mAh g^{-1} (86%) at 50 °C. These are the best rate performance reported to date for $LiMnPO_4$. This is ascribed to the morphology of the particles allowing rapid Li diffusion.

At higher rates, an increased difference in capacity between RT and 50 °C is observed. This kind of temperature-dependent effect was also reported in $LiFePO_4$ [19,20]. It ascribes to faster thermal motion at elevated temperature: i.e. Li diffusion is more rapid at the higher temperature. This confirms the influence of Li diffusion on rate performance, and explains the improved performance we observe using this platelet shaped material.

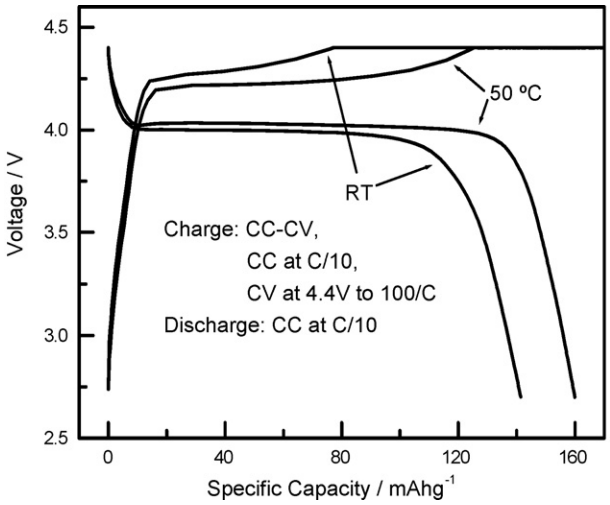

Fig. 4. The charge–discharge curves of our nano-$LiMnPO_4$/C composite at C/10.

The durability is also evaluated for our $LiMnPO_4$ at room temperature and 50 °C. At room temperature, polyol $LiMnPO_4$ material presented a good cyclibility (Fig. 6). The material at 199th exhib-

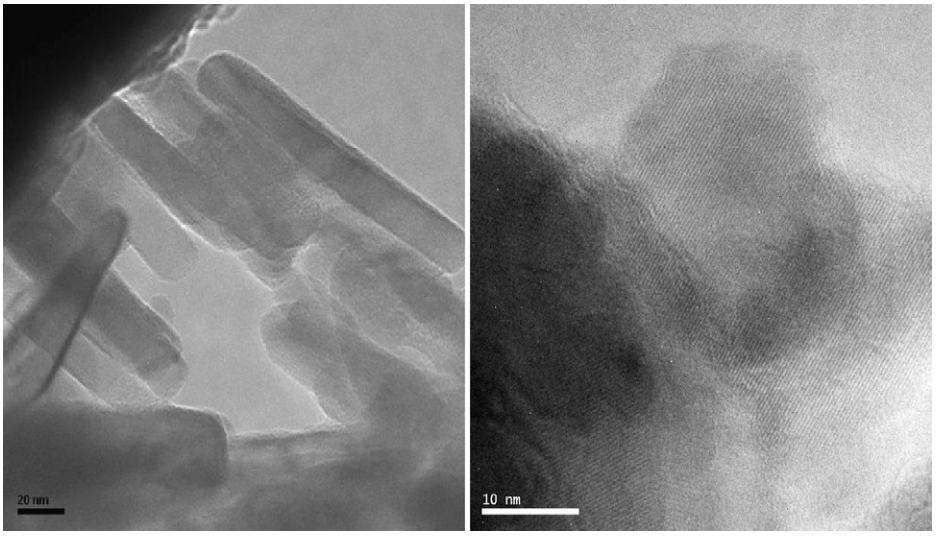

Fig. 3. TEM images of prepared sample.

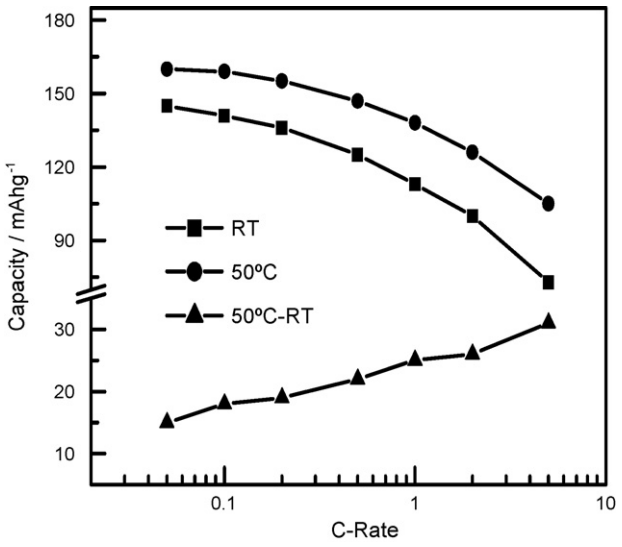

Fig. 5. The rate behavior of our material measured at room temperature and 50 °C.

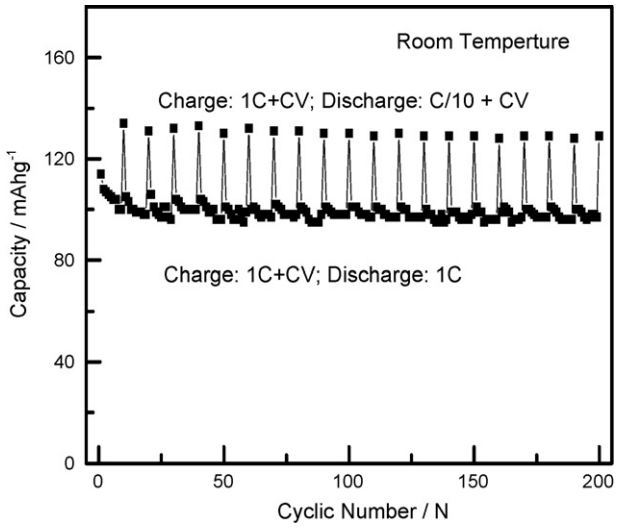

Fig. 6. The cyclic stability of our material tested at room temperature.

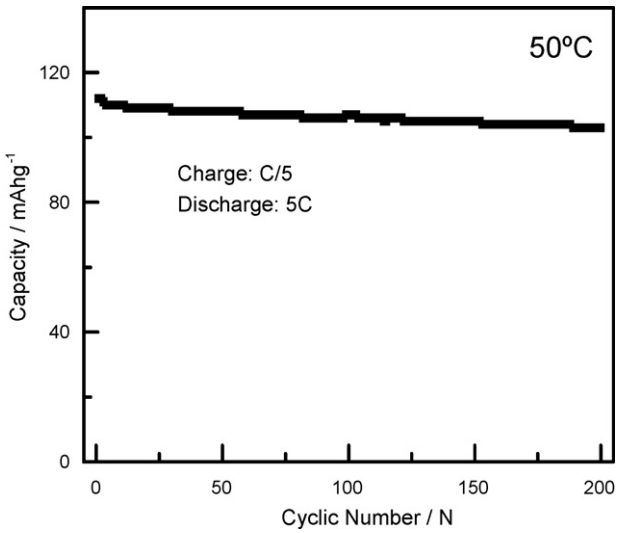

Fig. 7. The cyclibility of our sample measured at 50 °C.

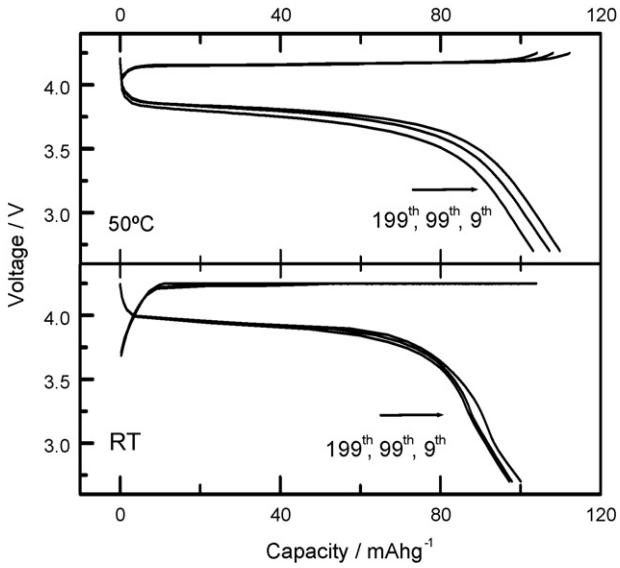

Fig. 8. Charge–discharge curves of 9th, 99th and 199th measured at room temperature and 50 °C.

ited ~97% capacity of 9th cycle. And it only lost ~5 mAh g^{-1} after 200 cycles. Moreover, the polyol $LiMnPO_4$ still shows a very stable cycle life at elevated temperature (Fig. 7). Its total fading capacity is only 9 mAh g^{-1} from 1st to 200th. For these tests we selected a lower charging cut-off voltage (4.25 V) in order to reduce the influence of solvent decomposition. In Fig. 8, we compared the charge–discharge curves of 9th, 99th and 199th at both temperatures. All selected curves in each system are almost superposed together. Fig. 9 presents the evolution of the specific capacity vs. rate, after 200 cycles at both temperatures. A small capacity fading capacity was observed, however the polarization remained similar. We ascribe this constant impedance to the stability of the electrolyte–$LiMnPO_4$ interface as reported by Martha et al. [18].

The observed stability, particularly at higher temperature, is due to the rigid three-dimensional structure that is stabilized by strong

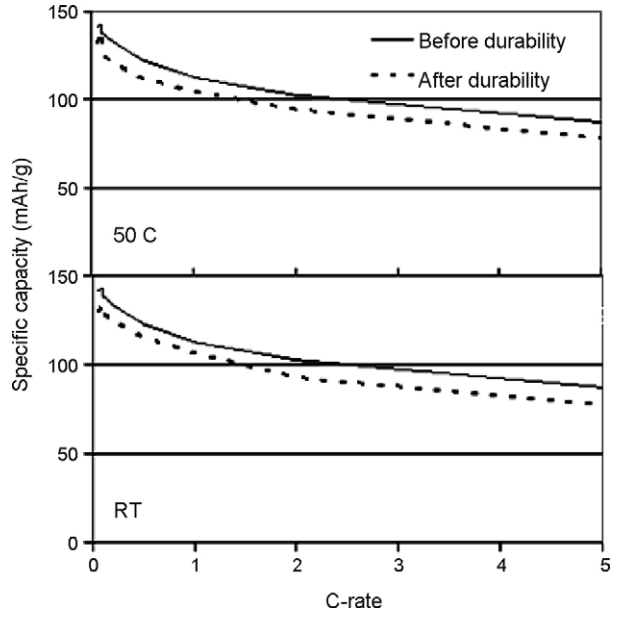

Fig. 9. Specific capacity of $LiMnPO_4$ vs. rate before and after 200 cycles at room temperature and at 50 °C.

covalent bonds between oxygen and the phosphorous ions. In addition, the nano-structured morphology of the polyol $LiMnPO_4$ may enhance its durability.

There has been much debate concerning the presence and function of Jahn–Teller distortion in $MnPO_4$. Jahn–Teller distortion is notorious in batteries field because it is one of the reasons for the unstable cycle life of spinel $LiMn_2O_4$ [21–24]. Tarascon predicted that orthorhombic $MnPO_4$ will endure a strong Jahn–Teller distortion [13]. However, our perfect cyclic performance formed a striking contrast to the very poor spinel. It implied that JT distortion plays a different role in $LiMnPO_4$, and may even stabilize the structure. Theoretical simulation is necessary for further explanation of this effect.

The results demonstrate that $LiMnPO_4$ demonstrates the same good durability as $LiFePO_4$.

4. Conclusion

We present a novel polyol method to synthesize high-performance $LiMnPO_4$. The material obtained from this method has presented the highest specific capacity among all published results: 145 mAh g^{-1} at C/20, 141 mAh g^{-1} at C/10 rate and 113 mAh g^{-1} 1C rate. The high rate performance is ascribed to the platelet morphology of the material which is only ~30 nm thick orientated in the *b* direction: giving a very short distance for Li diffusion.

The material exhibited a stable behavior at room temperature and 50 °C over 200 cycles. It is the first time to demonstration of the good cyclibility of $LiMnPO_4$. This cyclic data allows us to remove concerns of a negative influence of a Jahn–Teller distortion.

We conclude that $LiMnPO_4$ demonstrates the same good durability as $LiFePO_4$. This is ascribed to the strong bonds between oxygen and the phosphorous ions. In addition, the nano-structured morphology of the polyol $LiMnPO_4$ may enhance its durability. We demonstrate that its structure can stand a long-term cycling in spite of the existence of Mn(III) [d_4: $t_{2g}{}^3 e_g{}^1$].

These results prove that nano-structured materials achieved from novel synthesis methods can overcome transportation problems of the insulative-like $LiMnPO_4$. These results also prove $LiMnPO_4$ potential for performance and durability, and confirm in its promise as a cathode material for Li ion.

Acknowledgement

The authors really appreciate the useful discussions with Dr. Ouyang Chuying, who is working at the Department of Numerical Physics, Ecole Polytechnique Fédérale de Lausanne, Switzerland.

References

[1] A.K. Padhi, K.S. Nanjundaswamy, J.B. Goodenough, J. Electrochem. Soc. 144 (1997) 1188–1194.
[2] A. Yamada, S.C. Chung, J. Electrochem. Soc. 148 (2001) A960–A967.
[3] G.H. Li, H. Azuma, M. Tohda, Electrochem. Solid-State Lett. 5 (2002) A135–A137.
[4] M. Yonemura, A. Yamada, Y. Takei, N. Sonoyama, R. Kanno, J. Electrochem. Soc. 151 (2004) A1352–A1356.
[5] C. Delacourt, P. Poizot, M. Morcrette, C. Masquelier, Chem. Mater. 16 (2004) 93–99.
[6] N.H. Kwon, T. Drezen, I. Exnar, I. Teerlinck, M. Isono, M. Graetzel, Electrochem. Solid-State Lett. 9 (2006) A277–A280.
[7] T. Drezen, N.-H. Kwon, P. Bowen, I. Teerlinck, M. Isono, J. Power Sources 174 (2007) 949–953.
[8] H.S. Fang, L.P. Li, G.Sh. Li, Chem. Lett. 36 (2007) 436–437.
[9] H.S. Fang, L.P. Li, Y. Yang, G.F. Yan, G.S. Li, Chem. Commun. 9 (2008) 1118–1120.
[10] T.R. Kim, D.H. Kim, H.W. Ryu, J.H. Moon, J.H. Lee, S. Boo, J. Kim, J. Phys. Chem. Solids 68 (2007) 1203–1206.
[11] HPL patent, PCT/IB2006/051061.
[12] F. Fievet, J.P. Lagier, B. Blin, Solid State Ionics 32–33 (1989) 198–205.
[13] C. Delacourt, L. Laffont, R. Bouchet, C. Wurm, J.-B. Leriche, M. Morcrette, J.-M. Tarascon, M. Masquelier, J. Electrochem. Soc. 152 (2005) A913–A921.
[14] F. Zhou, M. Cococcioni, C.A. Marianetti, D. Morgan, G. Ceder, Phys. Rev. B 70 (2004), 2351211–8.
[15] A. Yamada, M. Hosoya, S.C. Chung, Y. Kudo, K. Hinokuma, K.-Y. Liu, Y. Nishi, J. Power Sources 119–121 (2003) 232–238.
[16] A. Yamada, Y. Takei, H. Koizumi, N. Sonoyama, R. Kanno, Chem. Matter. 18 (2006) 804–813.
[17] A. Yamada, Y. Kudo, K.-Y. Liu, J. Electrochem. Soc. 148 (2001) A1153–A1158.
[18] S.K. Martha, E. Markevich, V. Burgel, IMLB2008, J. Power Sources 189 (2009) 288–296.
[19] A.S. Andersson, J.O. Thomas, B. Kalska, L. Haggstrom, Electrochem. Solid-State Lett. 3 (2000) 66–68.
[20] M. Takahashi, S. Tobishima, K. Takei, Y. Sakurai, Solid State Ionics 148 (2002) 283–289.
[21] C.Y. Ouyang, S.Q. Shi, M.S. Lei, J. Alloy. Comp. 474 (2009) 370–374.
[22] R.J. Gummow, A. de Kock, M.M. Thackery, Solid State Ionics 69 (1994) 59–67.
[23] Y.Y. Xia, Y.H. Zhou, M. Yoshio, J. Electrochem. Soc. 144 (1997) 2593–2600.
[24] T. Eriksson, T. Gustafsson, J.O. Thomas, Electrochem. Solid-State Lett. 5 (2002) A35–A38.